Two physical mechanisms for boosting the quality factor to cavity volume ratio of photonic crystal microcavities

Ph. Lalanne, S. Mias, and J. P. Hugonin

Laboratoire Charles Fabry de l'Institut Optique, Centre National de la Recherche Scientifique et Université Paris Sud, BP 147, 91 403 Orsay Cedex, France.
Philippe.Lalanne@iota.u-psud.fr

Abstract: We identify two physical mechanisms which drastically increase the Q/V factor of photonic crystal microcavities. Both mechanisms rely on a fine tuning the geometry of the holes around the cavity defect. The first mechanism relies on engineering the mirrors in order to reduce the out-of-plane far field radiation. The second mechanism is less intuitive and relies on a pure electromagnetism effect based on transient fields at the sub-wavelength scale, namely a recycling of the mirror losses by radiation modes. The recycling mechanism enables the design of high-performance microresonators with moderate requirements on the mirror reflectivity. Once the geometry around the defect is optimised, both mechanisms are shown to strongly impact the Q and the Purcell factors of the microcavity.

OCIS codes: (130.3120) Integrated optics devices; (230.5750) Resonators; (230.6080) Sources; (250.5300) Photonic integrated circuits; (260.5740) Resonance; (140.5960) Semiconductor lasers

References and links

1. E.M. Purcell, "Spontaneous emission probabilities at radio frequencies", Phys. Rev. **69**, 681 (1946)
2. H. Yokoyama and K. Ujihara, *Spontaneous emission and laser oscillation in microcavities*, (FL: CRC Press, 1995)
3. O.J. Painter, A. Husain, A. Scherer, J.D. O'Brien, I. Kim, P.D. Dapkus," Room temperature photonic crystal defect lasers at near-infrared wavelengths in InGaAsP," J. Lightwave Technol. **17**, 2082-2088 (1999).
4. S. Noda, A. Chutinan and M. Imada, "Trapping and emission of photons by a single defect in a photonic bandgap structure," Nature **407**, 608-610 (2000).
5. D. Peyrade, E. Silberstein, P. Lalanne, A. Talneau, Y. Chen, "Short Bragg mirrors with adiabatic modal conversion," Appl. Phys. Lett. **81**, 829-831 (2002).
6. Y. Akahane, T. Asano, B-S Song and S. Noda, "High-Q photonic nanocavity in two-dimensional photonic crystal," Nature **425**, 944-47 (2003).
7. A.S. Jugessur, P. Pottier, R.M. De La Rue, "One-dimensional periodic photonic crystal microcavity filters with transition mode-matching features, embedded in ridge waveguides," Electron. Lett. **39**, 367-369 (2003).
8. M. Palamaru and Ph. Lalanne, "Photonic crystal waveguides: out-of-plane losses and adiabatic modal conversion," Appl. Phys. Lett. **78**, 1466-69 (2001).
9. Steven G. Johnson, Shanhui Fan, Attila Mekis and J. D. Joannopoulos, "Multipole-cancellation mechanism for high- Q cavities in the absence of a complete photonic band gap," Appl. Phys. Lett. **78**, 3388-00 (2001).
10. J. Vuckovic, M. Loncar, H. Mabuchi and A. Scherer, "Design of photonic crystal microcavities for cavity QED," Phys. Rev. **E 65**, art. #016608 (2002).
11. K. Srinivasan, O. Painter, "Momentum space design of high-Q photonic crystal optical cavities," Opt. Express **10**, 670-684 (2002), http://www.opticsexpress.org/abstract.cfm?URI=OPEX-10-15-670.
12. Ph. Lalanne and J. P. Hugonin, "Bloch-wave engineering for high Q's, small V's microcavities," IEEE J. Quantum Electron. **39**, 1430-38 (2003)
13. J.P. Zhang, D.Y. Chu, S.L. Wu, W.G. Bi, R.C. Tiberio, R.M. Joseph, A. Taflove, C.W. Tu, S.T. Ho, "Nanofabrication of 1-D Photonic Bandgap Structures Along Photonic Wire," IEEE Photon. Technol. Lett. **8**, 491 (1996).

#3583 - $15.00 US Received 23 December 2003; revised 29 January 2004; accepted 29 January 2004

14. J.S. Foresi, P.R. Villeneuve, J. Ferrera, E.R. Thoen, G. Steinmeyer, S. Fan, J.D. Joannopoulos, L.C. Kimerling, H.I. Smith and E.P. Ippen, "Photonic-bandgap microcavities in optical waveguides," Nature **390**, 143 (1997).
15. D.J. Ripin, K.Y. Lim, G.S. Petrich, P.R. Villeneuve, S. Fan, E.R. Thoen, J.D. Joannopoulos, E.P. Ippen and L.A. Kolodziejski, "Photonic band gap airbridge microcavity resonances in GaAs/AlxOy waveguides," J. Appl. Phys. **87**, 1578-80 (2000).
16. Ph. Lalanne and E. Silberstein, "Fourier-modal method applied to waveguide computational problems," Opt. Lett. **25**, 1092-94 (2000).
17. E. Silberstein, Ph. Lalanne, J.P. Hugonin and Q. Cao, "On the use of grating theory in integrated optics," J. Opt. Soc. Am. A. **18**, 2865 (2001).
18. J.P Bérenger, "A perfectly matched layer for the absorption of electromagnetic waves," J. Computational. Phys. 114, 185 (1994).
19. A.W. Snyder and J.D. Love, *Optical Waveguide theory* (Chapman and Hall, NY, 1983).
20. P. Benech and D. Khalil, "Rigorous spectral analysis of leaky structures: application to the prism coupling problem," Opt. Commun. **118**, 220 (1995).

1. Introduction

Electromagnetic resonant cavities, which trap light within a finite volume, are an essential component of many important optical devices and effects, from lasers to filters to single photon sources. Cavities are characterized by two main quantities: the modal volume V, and the quality factor Q. In many applications, high Q's and small V's are highly desirable for the high finesse required for laser and filter applications, and for the high Purcell factor [1] required for controlling the spontaneous emission of atoms placed in resonance with the microcavity mode [2]. For a dipole linewidth much smaller than the cavity linewidth, a simple derivation shows the Purcell factor is equal to $Q\,\lambda^3/(4\pi n^3 V)$, where n is the refractive index of the medium and λ is the resonant wavelength assumed to matched the emission wavelength. This formula holds for a perfect emitter placed at the antinode of the electromagnetic field and with its dipole parallel to the electric field. Thus the Purcell factor is a figure of merit of the cavity alone, which describes the cavity capability to enhance the spontaneous emission rate. At optical frequencies, due to the lack of good metals, the last decade has seen an intense research activity on a new generation of microresonator devices based on a three-dimensional engineering of the refractive index. Pure total internal reflection is used in spherical or disk-shaped resonators [2], whereas Bragg reflection in one or two dimensions (often with refractive confinement) is exploited in photonic-crystal microcavities like micropillars [2], photonic-crystal wires or two-dimensional photonic-band-gap waveguides [3-4].

In recent years, a variety of passive and active optical photonic-crystal microcavities has been constructed. It has been shown experimentally [5-7] and numerically [8-12] that a *fine* tuning of the geometry of the holes surrounding the cavity defect may *drastically* increase the cavity Q/V factor. In all the above references, the cavity performance has been improved by repeatedly adjusting the cavity parameters either during numerical simulation or during device fabrication. Many interesting concepts have been used for optimising the quality factors of the photonic crystal microcavities, including symmetry arguments [10], cancellation of the multipole far-field radiation [9], Bloch-wave engineering for increasing the modal reflectivity [8,12] or more recently "gently confining" light to avoid radiation [6,11]. Even so, it appears that the optimization of the quality factors of photonic crystal microcavities is indeed nontrivial and that the concepts behind it are not yet mature. A better understanding of the optimization techniques is highly valuable since three-dimensional computational loads are prohibitive.

In this work, we study the electromagnetic properties of one-dimensional photonic-band-gap air-bridge cavities (see Fig. 1(a)). Such microcavities have been studied previously [13-15], and Q factor of ≈ 300 (in good agreement with computational results) for $V \approx 0.03\ \mu m^3$ have been observed at telecommunication wavelengths. Although this in-line geometry appears conceptually more simple than some other two-dimensional photonic crystal geometries [6,10], we will show that its electromagnetic behavior is indeed unexpected and

#3583 - $15.00 US Received 23 December 2003; revised 29 January 2004; accepted 29 January 2004

intricate especially for small defect lengths. In Section 2, we interpret the physical origin of this novel unexpected behaviour through a modified Fabry-Perot model involving an energy recycling through leaky waves. To our knowledge, this phenomenon and its interpretation have not been previously discussed in the literature. In Section 3, two methods which rely on a fine tuning the geometry of the holes around the defect are proposed in order to increase the Q/V factor of the resonator by orders of magnitude. The first method relies on an optimisation of the recycling. The second method is based on a Bloch-wave engineering of the mirrors to reduce out-of-plane scattering. It has been previously discussed [12] but only for 2D geometries. As shown by numerical predictions obtained with a Fourier Modal method to solve exactly Maxwell's equations, both methods lead to Q values of $\approx 10^5$ with mode volumes approximately equal to the theoretical limit $(\lambda/n)^3$. Additionally, we show that these methods may be used for designing microcavities with high extraction efficiencies.

2. Cavity with fully periodic mirrors

Throughout this article, the computational results are obtained for a 340-nm-thick, 500-nm-wide air-bridge, as shown in Fig. 1(a). Unless otherwise mentioned, the periodicity constant and the hole-diameter are 450 nm and 250 nm, respectively. The semiconductor refractive index (n = 3.48) is assumed to be independent of the wavelength, an approximation largely inessential for the following discussion. In the wavelength range of interest, the waveguide supports a single TE-like mode (electric field primarily horizontal at the center of the waveguide) with a double mirror symmetry.

Figure 1(b) shows the calculated modal reflectivity of the mirror as a function of the wavelength, showing a large gap from λ = 1.4 to 1.9 μm. The reflectivity does not reach unity, and the deviation from 1 represents out-of-plane scattering losses because the modal transmission for four holes is negligeable. At mid-gap frequencies, ≈ 4% of light is scattered. The blue curve shows the cavity transmission spectrum for a defect length of h = 0.3 μm. The Q factor of the resonator is 1200, and the peak transmission at resonance is 25%. The three-dimensional computation is performed with a frequency-domain Fourier modal method [16-17]. In brief, the method relies on a supercell approach and incorporates Perfectly-Matched Layers [18] on the transversal side of the air-bridge. Since these layers absorb the evanescent and propagative radiation, the electromagnetic fields are null on every transversal boundaries of the supercell. Thus they are periodic functions of the transverse coordinates and can be extended into a Fourier series (plane-wave basis). This allows the calculation of the radiation and guided modes in a Fourier basis in each layer (the hole shapes are discretized in a series of thin uniform sections) and to use a scattering matrix approach to relate recursively the mode amplitudes in the different layers.

2.1 Unexpexted resonator behavior

Figure 1(c) shows the calculated transmission spectra of the cavity for default-length *h* varying from 0 to 1.5 μm. Within the gap of the mirrors, the transmission pattern exhibits a series of white fringes which correspond to cavity resonance. Examination of the fringe pattern reveals an intricate and unexpected behavior: the peak transmission at resonance of the second-order mode is abnormally high. For example, at mid-gap frequency, it is ≈50 times larger than that of the first-order, ≈30 times larger than that of the third-order and ≈20 times larger than the peak transmission T_{max} predicted with a Fabry-Perot model, $T_{max} = |t_m|^4/[1-|r_m|^2]^2$ [2], a value independent of the resonance order (t_m and r_m are the modal amplitude transmission and reflectivity of the photonic-band-gap mirrors). As we shall see hereafter, the Q factors associated with that resonance are also abnormally high. These computational results indicate that, although the Fabry-Perot model (commonly used in literature for the analysis of photonic crystal microcavities) well predicts the resonance locations in the (λ, *h*) plane when $\arg(r_m)+2\pi/\lambda\, n_{eff}\, h$ is a multiple of 2π, it largely misestimates the intricate resonance mechanism for small defect lengths. This is due to the fact that the Fabry-Perot model only considers modal quantities and completely ignores radiated fields. Intuitively, to

#3583 - $15.00 US Received 23 December 2003; revised 29 January 2004; accepted 29 January 2004

account for the factor of twenty times increase in the second-order-resonance peak transmission, one has to assume that the radiated field cooperates beneficially to the resonance mechanism.

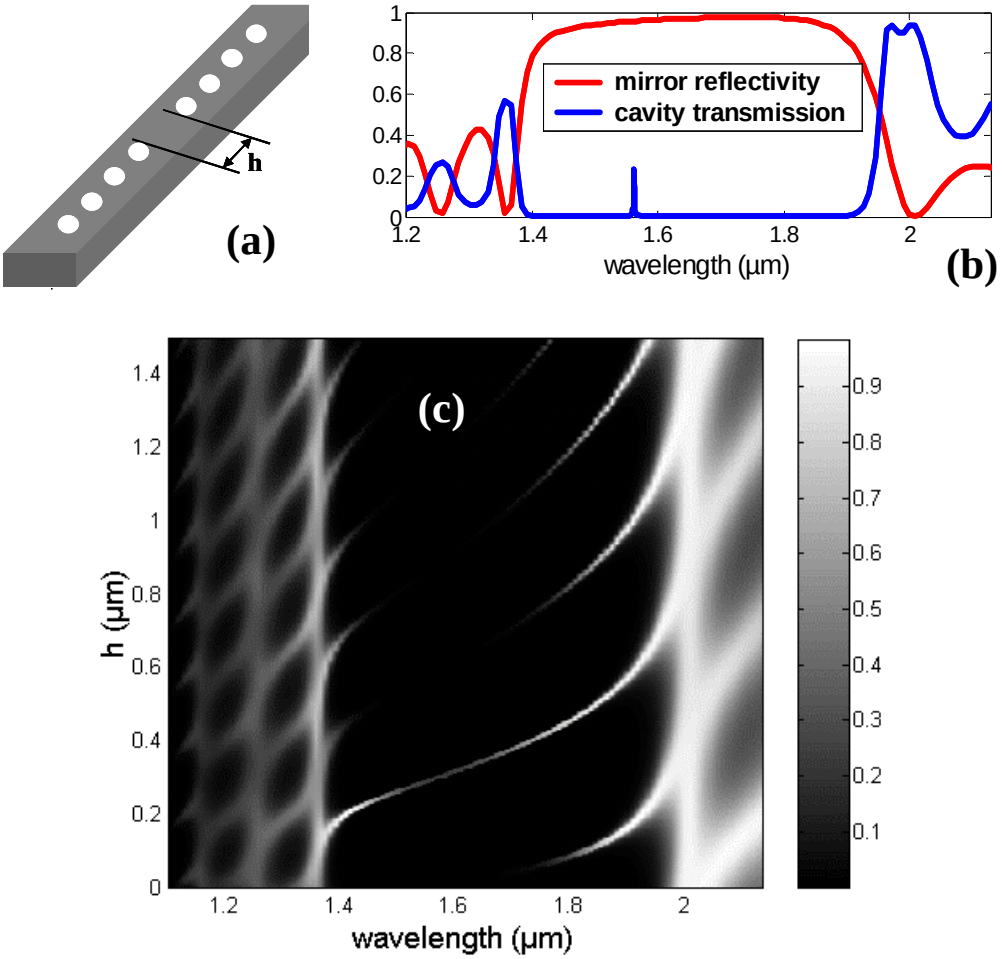

Fig. 1. (a) Air-bridge cavity geometry. The cavity is defined by two sets of four holes (diameter 250 nm, lattice constant 450 nm) separated by a defect of length h. The holes are assumed to be fully etched into a semiconductor (n = 3.48) air-bridge waveguide 340-nm thick and 500-nm wide. (b) Red curve : calculated modal mirror reflectivity spectrum. Blue curve : cavity transmission spectrum for h = 0.3 μm. (c) Calculated modal transmission as a function of wavelength and geometric cavity length h.

2.2 Radiation-loss recycling model

To support the above statement and to analyze the physical origin of the intricate resonance behavior, we have developed an analytical model with minimum parameters. Like for classical Fabry-Perot cavities, the model attributes the resonance to a phase-matching of the fundamental waveguide mode along one cavity cycle, but in addition, it encompasses a possible recycling of the radiated field. This recycling is taken into account within the model by introducing a leaky mode in the cavity resonance mechanism, as shown in Fig. 2. This representation is reasonable since leaky modes are powerful representations which are often sufficient for describing a portion of the total radiation field (in particular the portion close to the waveguide core) in many situations of practical interest [19], like prism-coupling into a surface-guide, coupling into hollow dielectric guides and scattering at Y-junctions in

#3583 - $15.00 US Received 23 December 2003; revised 29 January 2004; accepted 29 January 2004

integrated optics [20]. In the context of microcavities, they have not been previously studied to our knowledge. Referring to Fig. 2 and denoting by r' the reflection-coupling coefficient between the leaky mode and the fundamental mode, one easily obtains the master cavity equations

$$\alpha_1 = t_m + r_m \beta_1 + r' \beta_2 \quad (a)$$

$$\alpha_2 = r' \beta_1 \quad (b)$$

$$r = r'_m + t_m \beta_1 \quad (c)$$

$$t = t_m \alpha_1 \exp(i\phi_1) \quad (d)\ (1)$$

$$\beta_1 \exp(-i\phi_1) = r_m \alpha_1 \exp(i\phi_1) + r' \alpha_2 \exp(i\phi_2) \quad (e)$$

$$\beta_2 \exp(-i\phi_2) = r' \alpha_1 \exp(i\phi_1), \quad (f)$$

where ϕ_1 and ϕ_2 are the phase delays through the geometrical cavity length *h*. $\phi_1 = k_0 n_{eff} h$ and $\phi_2 = k_0(n'+in")h$, with n'+in" being the complex effective index of the leaky mode. In Eq. 1, α_j and β_j, j = 1 or 2, denote the amplitudes of the fundamental and leaky waves travelling to the right and to the left directions in the cavity. Under the assumption that the mirrors have symmetric refractive index profiles, $r'_m = r_m$ (reciprocity). Equations 1(a)-(f) are easily solved for the cavity modal transmission coefficient t and reflection coefficient r. Let us denote by r_{eff} the effective mirror reflectivity defined by

$$r_{eff} = r_m [1+2(r'/r_m)^2 \exp(i\phi_2 - i\phi_1)]^{1/2}. \quad (2)$$

If we assume that $|r'/r_m| << 1$ (i.e. $r_{eff} \approx r_m \approx 1$), an assumption valid for good mirrors, we find

$$t = \frac{t_m^2 \exp(i\phi_1)}{1 - r_{eff}^2 \exp(2i\phi_1)}, \quad (3)$$

and $r = r_{eff}[1+t \exp(i\phi_1)]$. Using the above assumption, the cavity reflection and transmission coefficients can be formally identified as those of a Fabry-Perot cavity whose mirror amplitude modal reflectivity and transmission coefficients are r_{eff} and t_m, respectively.

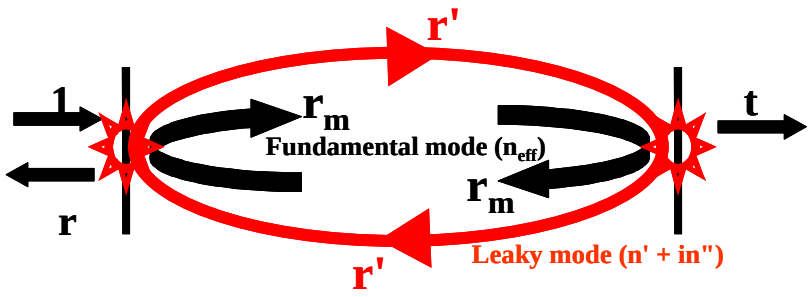

Fig. 2. Minimal model for recycling radiation in microcavities. Black and red arrows correspond to the fundamental and leaky modes, respectively. The cavity being symmetrical, the coupling coefficients r_m and r' are the same for both mirrors.

Let us now consider an isolated mirror illuminated by the fundamental guided mode with unit light intensity. This guided wave will be partly transmitted with an intensity $|t_m|^2$ and partly reflected with an intensity $|r_m|^2$. Due to the impedance mismatch between the fundamental Bloch mode supported by the mirror and the incident guided wave [8], a fraction $L = 1-|r_m|^2-|t_m|^2$ of the energy carried by the incident wave will also be radiated in the air cladding. If we denote by f the fraction of the radiation losses of the isolated mirror which can be potentially

#3583 - $15.00 US Received 23 December 2003; revised 29 January 2004; accepted 29 January 2004

recycled inside the cavity by the leaky wave ($f = |r'|^2 / L$), then the effective mirror reflectivity of Eq. (2) can be conveniently rewritten as

$$r_{eff} / r_m = 1+fL/|r_m|^2 \exp(-k_0 n'' h) \exp[ik_0(n'-n_{eff})h+2i\theta], \quad (4)$$

where $\theta = \arg(r'/r_m)$. By noting that $|r_{eff}|$ is maximum for $\theta = 0$ and $h = 0$, energy conservation for the cavity ($|r_{eff}|^2+|t_m|^2 < 1$) imposes an upper boundary for f, namely $f < 0.5$. The effective mirror reflectivity given by Eq. (4) is easily understood. For a cavity length *h*, the term $fL \exp(-k_0 n'' h)$ in Eq. (4) represents the fraction of the radiated energy recycled by the leaky mode and the argument of the last exponential term in Eq. (4) represents the phase shift over one-half cycle of the cavity between the fundamental mode and the recycled leaky mode. Depending on if these modes are phased matched or not, the recycling mechanism can be beneficial or detrimental for the resonator. For good cavities, the correction coefficient in Eq. (4) is small since $|r_m|^2 \approx 1$ and $fL \exp(-k_0 n'' h) << 1$. However, because the fundamental mode at resonance bounces many times inside the cavity, weak recycling takes place a great number of times and the cavity T_{max}, Q and F factors (as we shall see) are significantly increased.

2.3 Model validation

We have tested the model predictions against exact numerical results. Four independent real parameters (θ, n', n" and $f < 0.5$) have been estimated. Because a radiated field, i.e. a continuum of radiation modes, is likely not to be accurately represented by a single leaky mode, we have not performed a thorough estimation for these parameters. Figure 3 shows a comparison between exact calculated data and the model predictions for $\theta = 0.82\pi$, $f = 0.5$ and $n'+in'' = 0.5+i0.1$. n' is smaller than 1, consistent with the fact that the normalized propagation constant of a leaky mode is smaller than the refractive index of the cladding materials [19], air in our example. We emphasize that the model predictions are all obtained for the same set of parameters, a better agreement being achieved by incorporating a weak spectral dispersion for θ. In Fig. 3(a), we compare the T_{max} of the first five cavity orders for six frequencies covering the 400-nm-wide band-gap region. The model predictions (blue curves) are shifted horizontally by 0.05 for the sake of clarity. Clearly, the model well reproduces the intricate variations of T_{max} from one resonance to another. Other calculations not reported here and performed for other frequencies show similar agreement. The model is also able to predict accurately the impact of the recycling on the cavity Q. It is easily shown that the Q factor can be written as

$$Q = m\pi |r_{eff}|/(1-|r_{eff}|^2), \quad (5)$$

where m is the cavity order given by $m = 2n_{eff} h/\lambda - \lambda/\pi \, \partial[\arg(r_m)] /\partial\lambda - 2h \, \partial[n_{eff}] /\partial\lambda$. Figure 3(b) shows a comparison between the calculated Q's (circles) and the model predictions (bold curve) as a function of the number of holes N, for the second cavity order ($h = 0.326$) and for $\lambda = 1.56$ μm. The model predictions are obtained for the same set of parameters as in Fig. 3(a) and for $m = 3.0$, a value calculated with the Fourier modal method. For $N >> 1$, the intrinsic Q factor, predicted by the Fabry-Perot model and denoted Q_{FP} in the following, is simply $m\pi/L$, with $L = 1 - |r_m|^2$. At the mid-gap wavelength of $\lambda = 1.56$ μm, L = 4% and m = 3. Thus Q_{FP} is approximately 220, a value 8 times smaller than the actual Q value (Q = 1700). Clearly, the model well reflects the intricate behaviour of the microresonator, both for the Q factor and for the peak transmission at resonance.

3. Tuning hole-geometry around the defect for high Q/V

Two approaches, which can increase the cavity Q factor by several orders of magnitude while keeping the mode volume V of the cavity constant, are now considered. They are intrinsically different, but both rely on a fine tuning of the hole-geometry around the defect. The first approach (Section 3.1) uses the recycling mechanism described in the previous Section, while

#3583 - $15.00 US Received 23 December 2003; revised 29 January 2004; accepted 29 January 2004

the second approach (Section 3.2) consists in engineering the mirror to taper the guided mode into the mirror Bloch mode, thus decreasing losses [8,12].

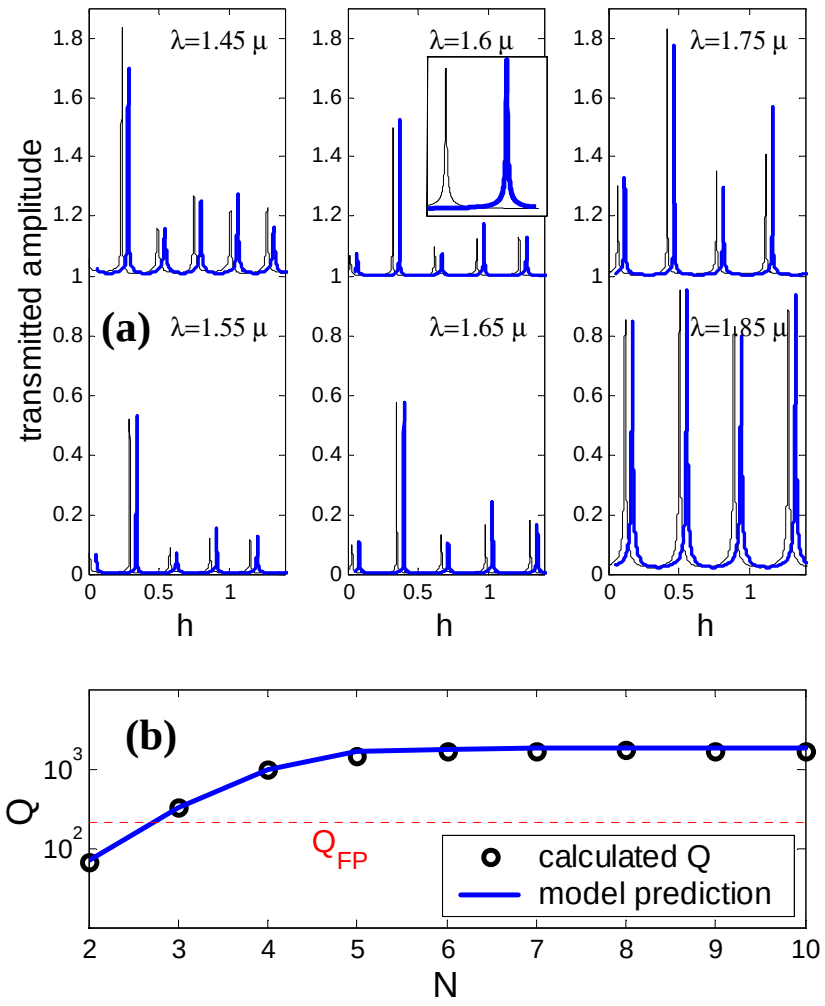

Fig. 3. Validation of the model. (a) Comparison between calculated data (black) and model predictions (blue) for the modulus of the cavity transmission coefficients |t| for six different wavelengths covering the full band-gap region. The t values for λ = 1.45, 1.6 and 1.75 μm values are vertically shifted by 1 and the model predictions are horizontally shifted by 0.05 (otherwise undistinguishable). The inset in the top center shows an enlarged view of the second resonance (h = 0.5 μm) (b) Q's as a function of the number N of holes for λ = 1.56 μm; black circles : calculated data, bold blue curve: model predictions. The horizontal dashed line represents the intrinsic Q_{FP} factor in the absence of recycling. For all curves, the model parameters are θ = 0.82π, f = 0.5 and n'+in" = 0.5+i0.1.

3.1 Recycling optimization

According to the model, the recycling is understood as a constructive interference between the fundamental and leaky modes. For a given resonance located in the (λ, *h*) plane by the Fabry-Perot condition $\arg(r_m)+2\pi/\lambda\, n_{eff}\, h = 0 \pmod{2\pi}$, a full recycling is expected if the argument $[k_0(n'-n_{eff})h+2\theta]$ of the exponential in Eq. (4) is a multiple of 2π. Because the effective-index

#3583 - $15.00 US Received 23 December 2003; revised 29 January 2004; accepted 29 January 2004

difference ($n'-n_{eff}$) is large for high index-contrast waveguides, only small modifications of the periodic-mirror geometry (i.e., small changes of $\arg(r_m)$ and θ) accompanied by small changes of *h* are likely to be sufficient for increasing further the recycling of the second-order cavity mode. In order to confirm this statement, we consider symmetric cavities formed by slightly varying the location of the two inner holes of the resonator and less importantly, their diameter.

Since the model is non-predictive concerning the details of the geometry, we performed calculations with the Fourier modal method for optimizing the Q factor. Figure 4 shows the transmission spectrum of an optimized geometry obtained for a 30-nm reduction of the hole-diameter and to a 70-nm outer displacement of the center hole-locations. In comparison with Fig. 1, much higher peaks are obtained for all cavity orders. This overall increase, which is not of special interest in the present context, is due to a better overlap between the fundamental mode and the Bloch mode of the photonic crystal mirror, and thus due to a reduction of the mirror losses L from 4% to 1.3% at mid-gap frequencies. This increase will be discussed in more detail in the next Section. More important for our current discussion is the beneficial impact of the recycling on the second cavity mode for which a ≈100% transmission is achieved at resonance over the full band-gap. This impact is especially remarkable when considering the cavity Q (see Fig. 5). While the classical Fabry-Perot model predicts an intrinsic Q_{FP} = 750 for the second cavity mode (m = 3.15) at λ = 1.56 μm, the calculated intrinsic Q is actually $\approx 10^5$. Thus for the engineered geometry, the recycling is responsible for an enhancement of the cavity Q by a factor 130. The large Q value mainly due to a strong recycling well compares with the highest Q values theoretically predicted so far for engineered two-dimensional PC geometries [6,10] and evidences the importance of the phenomenon for applications. Within the model picture, such an enhancement implies that 99 % of the radiated energy is effectively recycled.

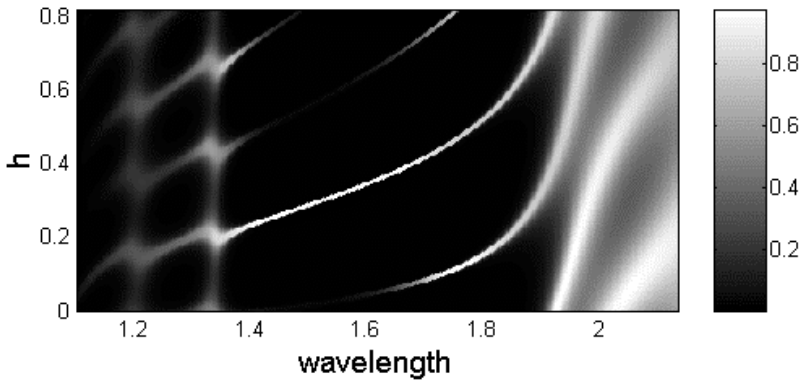

Fig. 4. Calculated modal transmission as a function of wavelength and cavity length h for the engineered cavity (N=4).

3.2 Modal reflectivity optimization

The previous optimisation allows for high Q/V ratios while working with moderate mirror losses in the range of 0.01. Hereafter, we consider another approach which provides a drastic Q/V improvement through a reduction of the mirror losses. No recycling is involved. In general terms, the far-field radiation at an interface between a z-invariant waveguide (the defect) and a z-periodic Bragg-mirror is due to the impedance-mismatch between the fundamental guided mode of the defect and the (non-propagating) fundamental Bloch mode of the Bragg mirror [8]. The radiation loss L varies linearly with the square of the overlap integral η between these two modes. Reducing these losses can be achieved by tapering the guided mode of the defect into the Bloch mode of the mirror. Details on the design of such a taper through Bloch-wave engineering can be found in [12].

#3583 - $15.00 US Received 23 December 2003; revised 29 January 2004; accepted 29 January 2004

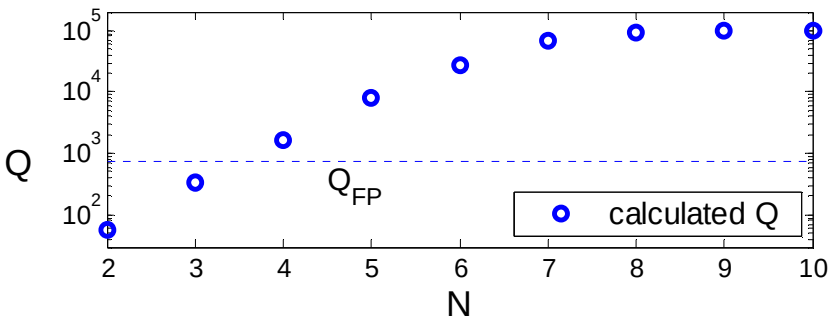

Fig. 5. Q factor as a function of the number of holes for the cavity with optimised recycling. Circles represent calculated data. The horizontal dashed line represents the cavity intrinsic Q_{FP} factor in the absence of recycling.

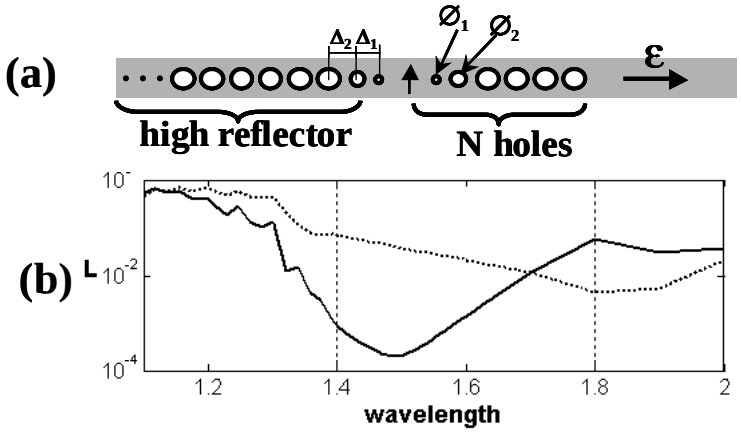

Fig. 6. Engineered mirrors. (a) Cavity with engineered mirrors. (b) Comparaison between the modal reflectivity spectra of a classical mirror (dotted curve) and that of the engineered mirror (solid curve). Vertical lines indicate the bandgap edges.

Figure 6(a) shows the cavity with tapered mirrors considered in the following. The high-reflectivity mirror has a constant number of holes (N' = 9, considered to have the same effect as an infinite number of holes) and incorporates a taper section consisting of two holes. The number of holes in the low-reflectivity mirror varies from 0 to 9 while a taper section is also incorporated. In this Section, the periodicity constant of the periodic section of the mirrors is reduced to 420 nm, while the associated hole-diameter is kept at 250 nm. This change is largely inessential and is motivated by future experimental characterization of devices. Through simulated annealing, we have optimized the hole-locations and diameters of the taper section. At $\lambda = 1.5$ μm, a minimum loss $L = 1-|r_m|^2-|t_m|^2$ is obtained for $\varnothing_1 = 100$ nm, $\varnothing_2 = 210$ nm and $\Delta_1 = 327$ nm, $\Delta_2 = 330$ nm (see Fig. 6(a) for a definition of the parameters). Figure 6(b) compares the radiation loss spectrum of the periodic mirror (dotted curve) with that of the tapered mirror (solid curve). At the design wavelength, a loss reduction by more than two orders of magnitude is achieved.

In Table 1, we compare the performance of the cavity with tapered mirrors with that of the cavity with periodic mirrors as a function of the number of holes N of the low-reflectivity mirror. The defect lengths *h* of the microcavities are chosen so that resonance occurs at $\lambda = 1.5$ μm (*h* = 635 nm and 557 nm, for the engineered and classical case, respectively). For all cases, we calculate the total power P emitted by a single-frequency ($\lambda = 1.5$ μm) linearly-

#3583 - $15.00 US Received 23 December 2003; revised 29 January 2004; accepted 29 January 2004

polarized dipole (see Fig. 6(a) for the dipole orientation) inserted at the center of the cavity defect. In experiments, this situation corresponds to a perfect emitter placed at the antinode of the cavity mode with an emission linewidth much smaller than the cavity linewidth. The Purcell factor F is derived by removing the small fraction of the dipole emission which is radiated into the background of the continuum of radiation states and by normalizing the emitted power to the total power emitted by the same dipole in the bulk material. In addition, we compute the extraction efficiency ε defined by the fraction of energy emitted through the low-reflectivity mirror into the air-bridge waveguide mode. High ε values are highly desirable in practice. For single-photon sources, ε represents the probability to emit one photon instead of none for a light pulse. As shown in Table 1, the cavity with engineered mirrors outperforms the one with classical mirrors both in terms of Q, F and ε.

Table 1. Cavity performance

	N	1	2	3	4	5
	Q	28	100	180	220	230
Classical	F	6.5	21	38	46	48
mirrors	ε	0.86	0.56	0.21	0.06	0.011
	Q	-	70	280	1300	5600
Engineered	F	-	10	40	190	800
mirrors	ε	-	0.96	0.98	0.96	0.88

4. Conclusion

A thorough study of the electromagnetic properties of in-line photonic-band-gap air-bridge cavities has revealed two physical mechanisms that can increase the Q/V factor of photonic crystal microcavities by several orders of magnitude. Both mechanisms rely on fine tuning the geometry of the holes around the cavity defect. The first mechanism relies on engineering the mirrors so as to reduce the impedance mismatch between the mirror and the waveguide defect and hence reduce the out-of-plane far field radiation. The second mechanism is less intuitive and in our opinion deserves further studies. It relies on a pure electromagnetism effect based on transient fields at the subwavelength scale, namely a recycling of the mirror losses by radiation modes and enables the design of high-perfomance microresonators with moderate requirements on the mirror reflectivities. Through an analytical model, we showed that the recycling mechanism obeys a phase-matching condition, and that, when appropriately optimised, it can boost the Q's and the Purcell factor by two orders of magnitude. We expect that these mechanisms may have an important impact on the ultimate performance of other photonic-crystal microcavity geometries [4-6,9-10]. In addition, these mechanisms may be useful for understanding some of the recent works on microcavities where a fine tuning of the geometry around the defect has had a large impact on the resonator performance.

Acknowledgments

We gratefully acknowledge P. Benech and J. M. Gérard for fruitful discussions. Solon Mias is with the Photonics and Sensors Group at Cambridge (UK). His research has been supported by a Marie curie fellowship of the European Community programme Information Optics: new Tools and Applications, contract n° HPMT-CT-2000-00105.